



**University of  
Zurich**<sup>UZH</sup>

**Zurich Open Repository and  
Archive**

University of Zurich  
University Library  
Strickhofstrasse 39  
CH-8057 Zurich  
[www.zora.uzh.ch](http://www.zora.uzh.ch)

---

Year: 2019

---

## Reconsidering Osteoconduction in the Era of Additive Manufacturing

Weber, Franz E

**Abstract:** Bone regeneration procedures in clinics and bone tissue engineering stand on three pillars: osteoconduction, osteoinduction, and stem cells. In the last two decades, the focus in this field has been on osteoinduction, which is realized by the use of bone morphogenetic proteins and the application of mesenchymal stem cells to treat bone defects. However, osteoconduction was reduced to a surface phenomenon because the supposedly ideal pore size of osteoconductive scaffolds was identified in the 1990s as 0.3-0.5 mm in diameter, forcing bone formation to occur predominantly on the surface. Meanwhile, additive manufacturing has evolved as a new tool to realize designed microarchitectures in bone substitutes, thereby enabling us to study osteoconduction as a true three-dimensional phenomenon. Moreover, by additive manufacturing, wide-open porous scaffolds can be produced in which bone formation occurs distant to the surface at a superior bony defect-bridging rate enabled by highly osteoconductive pores 1.2 mm in diameter. This review provides a historical overview and an updated definition of osteoconduction and related terms. In addition, it shows how additive manufacturing can be instrumental in studying and optimizing osteoconduction of bone substitutes, and provides novel optimized features and boundaries of osteoconductive microarchitectures. **Impact Statement** This review updates the definition of osteoconduction and draws clear lines to discriminate between osteoconduction, osseointegration, and osteoinduction. Moreover, additively manufactured libraries of scaffolds revealed that: osteoconduction is more a three-dimensional than a surface phenomenon; microarchitecture dictates defect bridging, which is the measure for osteoconduction; pore diameter or the diagonal of lattice microarchitectures of osteoconductive bone substitutes should be 1.2 mm.

DOI: <https://doi.org/10.1089/ten.TEB.2019.0047>

Posted at the Zurich Open Repository and Archive, University of Zurich

ZORA URL: <https://doi.org/10.5167/uzh-179263>

Journal Article

Published Version

The following work is licensed under a Publisher License.

Originally published at:

Weber, Franz E (2019). Reconsidering Osteoconduction in the Era of Additive Manufacturing. Tissue engineering. Part B, Reviews, 25(5):375-386.

DOI: <https://doi.org/10.1089/ten.TEB.2019.0047>

REVIEW ARTICLE

---

# Reconsidering Osteoconduction in the Era of Additive Manufacturing

Franz E. Weber, PhD<sup>1,2,3</sup>

Bone regeneration procedures in clinics and bone tissue engineering stand on three pillars: osteoconduction, osteoinduction, and stem cells. In the last two decades, the focus in this field has been on osteoinduction, which is realized by the use of bone morphogenetic proteins and the application of mesenchymal stem cells to treat bone defects. However, osteoconduction was reduced to a surface phenomenon because the supposedly ideal pore size of osteoconductive scaffolds was identified in the 1990s as 0.3–0.5 mm in diameter, forcing bone formation to occur predominantly on the surface. Meanwhile, additive manufacturing has evolved as a new tool to realize designed microarchitectures in bone substitutes, thereby enabling us to study osteoconduction as a true three-dimensional phenomenon. Moreover, by additive manufacturing, wide-open porous scaffolds can be produced in which bone formation occurs distant to the surface at a superior bony defect-bridging rate enabled by highly osteoconductive pores 1.2 mm in diameter. This review provides a historical overview and an updated definition of osteoconduction and related terms. In addition, it shows how additive manufacturing can be instrumental in studying and optimizing osteoconduction of bone substitutes, and provides novel optimized features and boundaries of osteoconductive microarchitectures.

**Keywords:** osteoconduction, microarchitecture, bone substitute, additive manufacturing, 3D printing, ceramics, osseointegration, osteoinduction

## Impact Statement

This review updates the definition of osteoconduction and draws clear lines to discriminate between osteoconduction, osseointegration, and osteoinduction. Moreover, additively manufactured libraries of scaffolds revealed that:

- osteoconduction is more a three-dimensional than a surface phenomenon;
- microarchitecture dictates defect bridging, which is the measure for osteoconduction;
- pore diameter or the diagonal of lattice microarchitectures of osteoconductive bone substitutes should be  $\sim 1.2$  mm.

## History of Osteoconduction

**T**HE RECOGNITION OF osteoconduction as an important driving force during bone regeneration is strongly associated with the use of allogeneic or xenogeneic bone as a bone substitute to fill a bony defect. In 1628, Meekeren reported in his book “*Observationes medicochirurgicae*”<sup>1</sup> the use of a canine bone to treat a skull defect in a Russian nobleman. Despite the successful treatment, the patient was not satisfied with the outcome because in the view of the church he was now dehumanized and therefore faced a choice between excommunication, which was a death sentence in those times, or removal of the xenogeneic material.<sup>2</sup>

Observations on osteogenesis and the importance of the periosteum were first reported in 1742 by Duhamel (as reviewed in Chase and Herndon<sup>3</sup>). Research on bone substitute materials, as we know it, started in the second half of the 18th century. At that time, Ollier performed research on bone regeneration, and introduced the terms autogeneic, allogeneic, and xenogeneic bone grafts<sup>4</sup> (Table 1). Profound knowledge regarding the fate of bone grafts was generated by histological studies by Barth published in 1893 and 1895.<sup>2,5</sup> He also coined the term: “*schleichender Ersatz*,” that is, creeping substitution, describing the gradual replacement of the bone transplant by newly formed bone based on neovascularization from the bony bed where the transplant was placed. The term

<sup>1</sup>Oral Biotechnology and Bioengineering, Center of Dental Medicine Department of Cranio-Maxillofacial and Oral Surgery, University of Zurich, Zurich, Switzerland.

<sup>2</sup>Center for Applied Biotechnology and Molecular Medicine (CABMM), University of Zurich, Zurich, Switzerland.

<sup>3</sup>Zurich Center for Integrative Human Physiology (ZIHP), University of Zurich, Zurich, Switzerland.

TABLE 1. TERMINOLOGY FOR BONE GRAFT OPERATIONS

<i>Noun</i>	<i>Adjective</i>	<i>Donor</i>
Autograft	Autogeneic	Same individual
Isograft	Isogeneic	Identical twin or inbred strain
Allograft	Allogeneic	Same species, living
Alloimplant	Allogeneic	Same species, dead
Xenograft	Xenogeneic	Another species

According to Barth.<sup>2</sup>

“creeping substitution” was established in the English-speaking world by Phemister in 1926.<sup>6</sup> The work of Barth was mainly based on histology, and was continued by Axhausen<sup>7</sup> on rabbit and rat samples and substantiated by human samples.

In 1914, an overview of the concept of bone grafts in surgery was read at the annual meeting of the Canadian Medical Association by Turner.<sup>8</sup> According to Turner, the three main theories of regeneration of bone by autografts at that time were (1) by G. Axhausen (1877–1960): “The bone in the graft always dies, is absorbed and reformed from periosteum, which alone remains living in transplants.”; (2) by W. McEwan (1848–1924): “The bone in a graft is reproduced from the proliferation of osteoblasts, derived from osteoblasts within the bone of the graft itself”; and (3) by J.B. Murphy (1857–1916): The “graft is not osteogenetic, but simply osteoconductive. Provided it be in contact at one or both extremities with other living bone, the graft acts simply as a scaffolding for the growth of the capillaries with their osteogenetic cells as they advance from the living contact extremities into the graft.” Therefore, it was J.B. Murphy before World War I who, most likely, coined the term osteoconduction, and certainly realized that osteoconduction was an important driving force for bone regeneration induced by autografts.

### Definition of Osteoconduction and Closely Related Terms

#### *Osteoconduction*

Osteoconduction is defined as a three-dimensional (3D) process of ingrowth of sprouting capillaries, perivascular tissue, and osteoprogenitor cells from a bony bed into the 3D structure of a porous implant (adjusted from Cornell and Lane<sup>9</sup>; Urist<sup>10</sup>) used as a guiding cue to bridge a defect with bony tissue.

This implies that osteoconduction is a 3D phenomenon, and that biological readouts for osteoconduction are the velocity of bone ingrowth into 3D structures or the bony bridging of a defect,<sup>11,12</sup> a notable diagnostic feature of nonunions. This underlines the directional aspect of osteoconduction as a guiding cue to avoid nonunions. As stated by Urist,<sup>10</sup> “Osteoconduction occurs within a framework of nonbiologic materials such as glass, ceramics, and plastics, as well as within nonviable biologic materials such as autoclaved bone, deproteinized bone, demineralized-trypsinized bone, and frozen or freeze-dried allogeneic bone.

In nonbiologic frameworks, osteoconduction may occur without resorption of the underlying framework. In nonviable biologic frameworks, osteoconduction may occur with or without resorption of the implanted material. In a viable bone autograft, osteoconduction is facilitated by osteoinductive

processes and is more rapid than osteoconduction by non-biologic materials.” Because osteoconduction occurs independently from osteoinductive factors originating from the scaffold, it is the main driving force for bone regeneration for nonviable and synthetic bone substitute scaffolds.

#### *Osseointegration*

Osseointegration is defined as establishment of a direct contact between implant and bone achieved, and maintained, during functional loading (adjusted from Albrektsson *et al.*<sup>13</sup>; Branemark *et al.*<sup>14</sup>).

Osseointegration appears as more of a two-dimensional (2D) surface phenomenon, and describes the direct contact between the surface of an implant and bone. Its biological readout is percentage of bone-to-implant contact or the forces needed to remove the implant from the bone. The rigid fixation of an implant in orthopedic praxis can be determined using radio-stereophotogrammetric techniques and, at least in craniofacial implantology, resonance frequency analysis.<sup>15</sup> Osseointegration is of great importance for dental implants, which are primarily made from titanium. Moderately rough surface topographies of dental titanium-based implants, which can be achieved by surface etching and sandblasting, appear to be optimal for osseointegration at the micro- and nanolevel.<sup>16–18</sup> This can reflect preferential binding of blood components due to optimal combination of nanostructures and hydrophilicity on the surface.<sup>18–20</sup>

#### *Osteoinduction*

Osteoinduction is defined as the induction of undifferentiated mesenchymal stem cells that are not yet committed to the osteogenic lineage to form osteoprogenitor cells and to produce bone at heterotopic sites (adjusted from Urist<sup>10</sup>; Barradas *et al.*<sup>21</sup>; Friedenstein *et al.*<sup>22</sup>).

Osteoinduction, in contrast with osteoconduction and osseointegration, is not restricted to bony beds but acts also at ectopic sites, such as in subcutaneous pouches in animal models. Therefore, the biological readout for osteoinduction is the extent of bone formation at an ectopic site. Levander observed osteoinduction in 1934 when he injected crude alcoholic extracts of bone into muscles.<sup>23,24</sup> The search for the bone inducing principle started with the groundbreaking observations by Urist in 1965,<sup>25</sup> describing normal bone formation in the form of ossicles, after implantation of demineralized bone matrix in soft tissues of rabbits, rats, mice, and guinea pigs. These observations finally led to the discovery and cloning of bone morphogenetic proteins (BMPs),<sup>26</sup> which have been used clinically in the form of human recombinant BMP-2 since the beginning of this century.<sup>27</sup>

BMPs and therefore osteoinduction play an essential role in any bone formation activity. BMPs are secreted by osteoblasts and deposited in the bone matrix to coordinate bone remodeling.<sup>28</sup> Osteoinduction has also been seen with hydroxyapatite-based scaffolds at ectopic sites without the addition of BMPs.<sup>29</sup> One can speculate that endogenous BMPs in circulation bind to the hydroxyapatite disk and that at a certain biological threshold of bound endogenous BMPs, the formerly osteoconductive scaffold gradually acquires osteoinductive features.<sup>30</sup> In a more recent study with tricalcium phosphate (TCP), different sintering temperatures induced changes in microporosities correlated with osteoinductive potential in muscle pouches of dogs.<sup>31</sup> Overall,

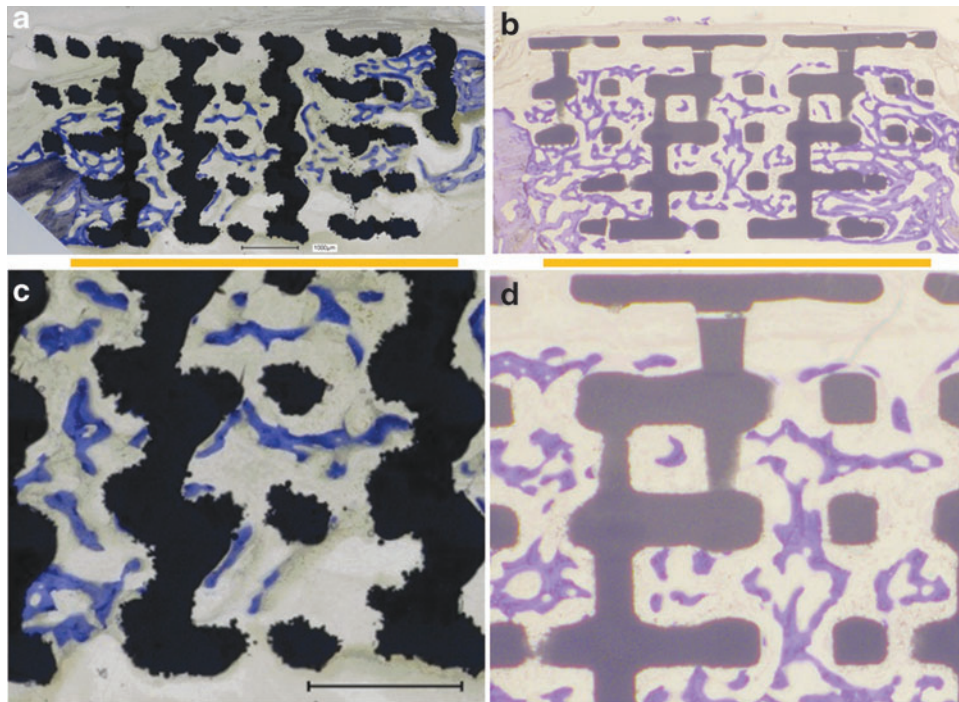


**FIG. 1.** Histological sections from the middle of the defect from one exemplary animal 4 weeks postoperative. (a) Titanium implant, (b) TCP implant. The yellow line underneath indicates the defect margins. (c) Higher magnification from (a). (d) Higher magnification from (b). Scale bars in (a) and (c) indicate 1 mm, and apply to (b) and (d) as well. Bone appears as grayish purple to blue. (a) and (b) are derived from Chen *et al.*<sup>99</sup> with permission. TCP, tricalcium phosphate.

topography, concavities, composition, macropore size, percent porosity, and microporosities can tune calcium-phosphate-based scaffolds toward osteoinduction.<sup>32</sup> For concavities, it appears that 90 days after implantation, differentiating osteoblast-like cells reside in the concavities, and secrete and embed osteogenic molecular signals, such as osteogenic protein-1 (BMP-7), into these smart concavities.<sup>33</sup> However, definitive evidence of the enrichment of circulating BMPs on calcium phosphate-based scaffolds is still elusive.

Moreover, notably, these scaffolds were tested and found useful in muscle pouches but failed in subcutaneous pouches. Therefore, this osteoinductivity could depend on the proximity to muscle-derived mesenchymal stem cells and mechanical interactions between the rigid scaffold and the muscle fibers, which could induce repair mechanisms in the muscle, including migration of muscle-derived mesenchymal stem cells to the implanted scaffold.<sup>34</sup> However, in bone defects, these osteoinductive calcium-phosphate-derived scaffolds were shown to perform better than nonosteoinductive scaffolds with lower microporosities<sup>31</sup> and appear to be a promising material for bone substitutes. However, thus far commercial enterprises that based their products on this technology have failed in the market. Whether the superior performance of these osteoinductive calcium-phosphate-derived scaffolds in bony beds is due to binding of circulating autologous BMP to microporosities has neither been proven nor dismissed up to now.

#### Osteoconduction and Surface of the Implant

Osteoconduction, defined as directed bone ingrowth into the voids of a porous scaffold to close a bony defect, is best illustrated in Figure 1 for wide-open porous scaffolds constructed from titanium and TCP. For both titanium (Fig. 1a, c) and TCP (Fig. 1b, d) materials, the bone formed between the rods and barely on the surface of the rods when growing through the empty space in a scaffold placed in a noncritical

cranial defect in rabbits. Thus, for osteoconduction to occur, the rods of the scaffold serve as guiding cues to direct bone growth and close the bony defect even without physical contact between the newly formed bone and the material.

Therefore, osteoconduction can best be illustrated and studied with wide-open porous scaffolds because bone growth in channels of  $\leq 0.4$  mm occurs on the channel walls,<sup>35</sup> and the influence of the material and its surface on bone ingrowth might become more prominent. This notion is supported by the slowdown of bone ingrowth in lattice structures with a rod distance of 0.3 mm compared with a rod distance of 0.8 mm. For a rod distance of 0.8 mm, the defect was  $90.83 \pm 16.22\%$  bridged, compared with a rod distance of 0.3 mm, where to only  $57.50 \pm 24.57\%$  bony bridging occurred.<sup>36</sup>

This suggests that bone ingrowth is significantly faster, and thus osteoconduction is optimized in wide-open microarchitectures compared with narrower counterparts,<sup>36</sup> and that the surface component overpowers osteoconduction in narrow structures. The results from narrow microarchitectures might be the reason for a definition of osteoconduction as provided in a previous study<sup>15</sup>: “This term (osteoconduction) means that bone grows on a surface.” Such a definition reduces osteoconduction to a 2D phenomenon, loses sight of the strong 3D and guiding contribution associated with osteoconduction, and might only apply to less osteoconductive scaffolds with narrow porous systems.<sup>35</sup>

Others have linked osteoconduction to osseointegration, and defined it as “the recruitment and migration of osteogenic cells to the implant surface.”<sup>37</sup> In the author’s view, this is also a misguided use of the term osteoconduction and describes the early stages of osseointegration. From our experience with wide-open porous structures, the woven bone (purple in Figure 2), which forms first, is deposited between and preferentially distant to the titanium rods. The lamellar bone, which forms next and on top of the woven bone (grayish in Fig. 2), is deposited in layers toward the



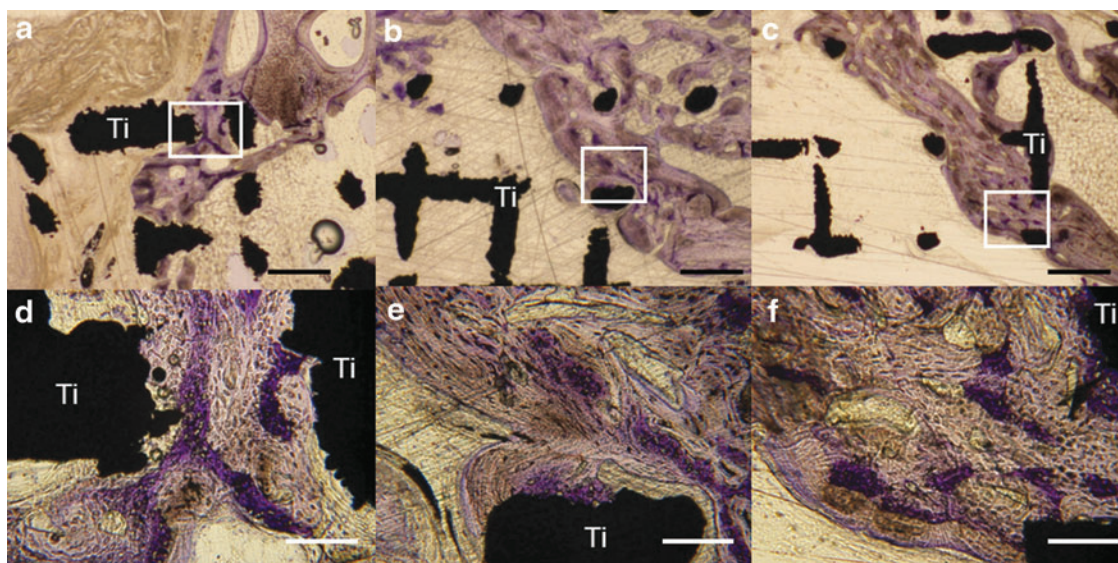


**FIG. 2.** High-magnification images of histological sections from the middle of the defect 8 weeks postoperative. Titanium implant with a (a, d) native selective laser melted (SLM), (b, e) sandblasted SLM, and (c, f) sandblasted and acid-etched SLM surface. The white square indicates the location of the related higher magnification picture in the lower panel. Black scale bars (upper panel) indicate 500  $\mu$ m; white scale bars (lower panel) indicate 100  $\mu$ m. Original magnifications were 200 (a–c)- and 1000 (d–f)-fold. Titanium (black) is indicated by Ti. The grayish-stained bone tissue is lamellar bone (also new but formed later) on the initial woven bone structures stained purple. Figure is reproduced with permission from de Wild *et al.*<sup>38</sup>

titanium scaffold. This indicates that the initial bone formed in the scaffold barely touches the scaffold but uses it more indirectly as 3D guiding cue to close the bony defect. Thus, osteoconduction in wide-open porous structures refers to woven bone growing through a scaffold. Only in the next phase is the scaffold osseointegrated to some extent, primarily by lamellar bone formed in layers on top of the initially deposited woven bone.

In essence, for wide-open porous structures, bone growth into the scaffold occurs predominantly between the rods and barely on the surface of the rods. This could be the reason why surface optimization of wide-open titanium lattice structures, ranging from selective laser-melted surfaces to sandblasted and sandblasted acid-etched titanium scaffolds, had no significant influence on defect bridging.<sup>38</sup> One could speculate that the influence of the surface on osteoconduction for wide-open scaffolds is reduced compared with narrow structures. This notion is supported by results from tunnel systems of different diameters in hydroxyapatite scaffolds, where bone grew on the walls of the tunnels until a diameter of 0.4 mm. At diameters of 0.5 and 0.6 mm, bone started to grow in the middle of the tunnels<sup>35</sup> without direct exposure to the surface of the material. These numbers should also represent the lower limit for wide-open microarchitectures.

### Osteoconduction and Microarchitecture

The macroarchitecture of a scaffold is defined as its overall outer shape. Its inner microarchitecture comprises pore size, shape, porosity, spatial distribution, channels, and pore interconnection, and its nanoarchitecture includes the inner and outer surfaces. Nanoarchitecture is determined by the production methodology or by the surface modifications applied after the initial production procedure.<sup>39–41</sup> In the context of bone regeneration, the micro-

architecture of cancellous bone, with its large surface area, was found to be superior to that of cortical bone because it has a greater potential for forming new bone.<sup>42,43</sup> Therefore, reproduction of cancellous bone-mimicking structures was attempted during the development of synthetic bone substitutes; for example, through a search for similar natural structures, such as the exoskeleton of marine species.<sup>44</sup> This is certainly a major misconception in the search for the most osteoconductive microarchitecture because the microarchitecture of cortical bone reflects the local mechanical needs,<sup>45</sup> and thus, no evolutionary pressure exists on osteoconduction in terms of bone ingrowth into 3D structures.

For wide-open porous titanium-based structures, no significant difference exists between the more “artificial” lattice and the more “natural” porous structures.<sup>41</sup> This suggests that the search for osteoconductive microarchitectures should not be limited to natural porous structures but can encompass any microarchitecture generated *in silico*<sup>46</sup> with computer-aided design software.

Osteoinduction in a rat ectopic model through delivery of BMP-2 through solid or porous hydroxyapatite particles illustrated the necessity for porosity in bone formation.<sup>47</sup> The porosity of 3D biomaterial scaffolds and osteogenesis has been reviewed extensively.<sup>48</sup> More recent studies reported on bone ingrowth and the presence of cells in micropores well <0.1 mm in diameter.<sup>49–51</sup> However, the minimum recommended pore size for bone substitute scaffolds is 0.1 mm,<sup>52</sup> but was suggested to exceed 0.3 mm in diameter.<sup>48</sup> An extended study with several TCP-based scaffolds with macropores of 0.15 mm in diameter showed no difference between diverse microporosities.<sup>53</sup> Therefore, the question of the influence of microporosities on osteoconduction has not yet been answered.

In textbooks and review articles, a pore diameter of 0.3–0.5 mm has long been regarded as the optimal size for

osteoconduction, enabling efficient Haversian type<sup>47</sup> and trabecular<sup>32</sup> bone formation. An optimal pore dimension of 0.2–0.5 mm is also supported by several *in vitro* studies (reviewed in Perez and Mestres<sup>54</sup>), although *in vitro* studies poorly reflect the situation in a bony bed, which is a prerequisite for osteoconduction to occur. Two *in vivo* studies, which set the optimal pore size between 0.3 and 0.4 mm, used an osteoinduction instead of an osteoconduction *in vivo* model.<sup>35,55</sup> Since osteoinduction can overwrite osteoconduction, these results should not be used to define the optimal pore size for an osteoconductive microarchitecture.

There are reports that bone substitutes with pore sizes in excess of 0.4 mm are less conducive to new bone formation.<sup>55</sup> In such a report, osteoconduction was tested in cortical windows of proximal tibias in rabbits with hydroxyapatite-based scaffolds, featuring parallel cylindrical pores of various sizes from 0.05 to 0.5 mm diameter without any interconnecting fenestration between adjacent pores. Here, the most favorable dimension was with channels 0.3 mm in diameter. However, the comparison was not based on defect bridging but on an increase in compression strength after an 8-week period.<sup>56</sup>

In contrast to porous or open-porous microarchitectures, single channels of defined diameters without interconnections present a situation of limited nutrient supply and insufficient waste removal, and might not be the ideal test system to define the most osteoconductive microarchitecture. Therefore, in the view of the author, the conclusion based on single channels, specifically, that pore sizes in excess of 0.4 mm are less conducive is ill suited to define the upper limit of an osteoconductive pore size. Larger pores with wide-open interconnections are certainly more favorable for nutrient supply and waste removal within the scaffold, first through diffusion and later on through vascularization. However, a guiding component of the scaffold central for osteoconduction might yield a natural limitation of the osteoconductive pore size irrespective of its influence on the mechanics of the scaffold.

Additional conflicting results concerning diverse materials and optimal pore size for osteoconduction are provided in this paragraph. A long-term study was performed with tantalum-based scaffolds with interconnected pores of 0.43 and 0.65 mm. At 4 weeks, bone ingrowth into the scaffolds was significantly better with larger pores. However, at 52 weeks, the scaffold with smaller pores showed better ingrowth.<sup>57</sup> In another study, biphasic calcium phosphate ceramic scaffolds were implanted into a distal femoral site in rabbits to compare pores of 0.36 mm with pores of 0.56 mm, and the larger pores were found to be more beneficial.<sup>58</sup> In contrast, when poly(propylene fumarate)-based scaffolds with pores between 0.3 and 0.5 mm and pores between 0.6 and 0.8 mm were tested in a calvarial defect model in rabbits, no significant difference could be observed in inflammation and bone formation.<sup>59</sup>

Porous titanium-based scaffolds fabricated by vacuum diffusion bonding of titanium meshes with pores of 0.188, 0.313, and 0.390 mm in diameter have been tested for bone ingrowth. In an *in vitro* test for cell ingrowth and cell proliferation, the smallest (0.188 mm) pores performed best. However, *in vivo*, the most extended (0.390 mm) pores outperformed the smaller ones,<sup>60</sup> illustrating that bigger pores are superior *in vivo*, and that *in vitro* results on osteoconduction do not reflect the *in vivo* outcome. It is undisputed that implant surfaces play important roles in regulating protein adsorption and deter-

mining subsequent cell responses, including cell attachment, proliferation, migration, and differentiation.<sup>61</sup> However, *in vitro* studies with cells have suggested osteoconductive potential of surfaces, contradicting *in vivo* results.<sup>62,63</sup> This is reasonable because the prerequisite for osteoconduction involves placement of the scaffold in a bony bed and additional features, such as vascularization, which are presently lacking in currently available *in vitro* systems.

In essence, the presently available *in vitro* systems are not suited to study osteoconductive microarchitectures. Moreover, the majority of *in vivo* studies have been performed with scaffolds containing randomly distributed pores and undefined interconnectivities, and some have utilized osteoinduction by BMPs to study bone ingrowth,<sup>35,47,55</sup> which could interfere or even disturb osteoconduction. In the vast majority of reports on osteogenesis and pore size, the pores were <0.5 mm in diameter, and thus did not include a wide-open microarchitecture. There is only one *in vivo* study with different scaffolds containing pores from 0.5 up to 1.2 mm, showing that bone ingrowth was independent of pore diameter in this range.<sup>64</sup> The limitations of this study were that scaffolds with pores >1.2 mm were not tested, the distribution of the pores in the scaffolds was random, and their interconnection undefined.

Therefore, all the examples given in this chapter provide some insight into osteoconductive, pore-based microarchitectures. However, overall, these results were based on many different materials and diverse *in vivo* systems, and thus, even if taken together, they fail to produce a comprehensive overview of osteoconduction as a phenomenon.

One reason for this puzzling picture of osteoconduction in the literature is certainly limitations in the production methodologies to produce a library of defined microarchitectures to test for osteoconduction in a more systematic manner. In one study, the mold to generate tubular microarchitectures with pores of 0.5 mm was produced by additive manufacturing. In a tibial defect model, this scaffold performed significantly better than the traditional random porous microarchitectures.<sup>65</sup> Therefore, additive manufacturing appears to be the tool of choice to produce libraries of scaffolds with diverse microarchitectures and to systematically study the effect of microarchitecture on osteoconduction.

### Osteoconduction and Microarchitectures Derived from Additive Manufacturing

The effectiveness of 3D printing as an additive manufacturing technique in regenerative medicine, particularly bone tissue engineering, has been extensively reviewed,<sup>66–68</sup> as have the diverse additive manufacturing methodologies.<sup>69</sup> However, studies of the relationship between microarchitecture and osteoconduction are rather limited in number.<sup>70,71</sup> Additive manufacturing, in contrast to subtractive methodologies, creates an object layer by layer. Examples of additive manufacturing methodologies are stereolithography, selective laser sintering,<sup>72</sup> and 3D printing in a powder bed.<sup>73</sup> The latter has been applied for ceramics to build bone substitutes.<sup>74,75</sup> Melt-extrusion additive manufacturing was established in 1992<sup>76</sup> and solution/slurry/gel extrusion in 2002.<sup>77,78</sup> In all extrusion-based methodologies, a polymeric filament is extruded through a nozzle and deposited layer by layer on a building platform. This also applies to fused deposition

modeling with poly-ε-caprolactone.<sup>79,80</sup> All filament-based additive manufacturing methodologies have the disadvantage that the resulting microarchitecture is highly dependent on the dimension and the mechanical constraints predefined by the filament at the time point of extrusion. In the majority of examples, the pore size in the *x*, *y*-axis equals the distance between the filaments. Here, the distance has to be in line with the mechanics of the filament just after extrusion to prevent the filament from bending or even collapsing onto a lower building level (Fig. 3b, c). In the *z*-axis, the pore diameter is predefined by the thickness of the filaments, and if not, multiple layers of filaments are deposited on top of each other.

Overall, filament-based additive manufacturing very much constrains the variability of the microarchitecture, and appears less suited to study the relationship between osteoconduction and microarchitecture in detail. This does not imply that a filament-based 3D printing approach could not be used to produce the best osteoconductive microarchitecture in the future. However, in the search for an ideal osteoconductive microarchitecture, lithography-based additive manufacturing methodologies might be the best suited to study microarchitecture and osteoconduction due to their high resolution (the layer thickness can be set as low as 0.04 mm and the *x*-*y*-resolution even smaller<sup>81</sup>) and the greater design freedom.

Early studies on polylactide-based scaffolds produced by 3D techniques showed worse bony bridging than seen with negative controls; that is, the empty defect.<sup>82</sup> When the same design was realized with hydroxyapatite-based scaffolds, osteoconduction with the scaffolds slightly exceeded bony bridging in the empty defects.<sup>83</sup> However, the radial pores in this design had a dimension of  $1.6 \times 1.0$  mm, which might have been too large for osteoconduction to occur efficiently.<sup>84</sup> Overall, this result suggests that the

choice of material and its associated possible degradation products can influence or even overwrite osteoconduction. Therefore, microarchitectures should be studied with slow degrading or nondegrading materials, such as calcium phosphates or titanium.

Titanium has been used extensively as a bone substitute due to its biocompatibility and mechanical strength, although it lacks biodegradability. *In vivo* tests with scaffolds containing pores between 0.30 and 0.90 mm illustrated that the scaffold with the smallest pore size showed reduced bone ingrowth.<sup>85</sup> In another study, a scaffold with 0.6 mm pores performed slightly better than ones with 0.9 mm pores.<sup>86</sup> These results have also been observed by others,<sup>87</sup> looking at a similar array of pore dimensions.

In a more recent report, porous titanium implants produced by selective laser melting were tested in a sheep long bone *in vivo* model. The diamond-shaped unit cells had dimensions of 0.6, 0.9, and 1.2 mm. Unfortunately; the strut size between the unit cells differed between the structures and reduced the open pores to <0.4 mm. Here, a unit cell of 0.9 mm showed the best bone ingrowth.<sup>88</sup> Pores 3.2 mm in diameter were used for honeycomb-shaped meshes to generate mechanobiologically optimized configurations for scaffolds to successfully treat large bone defects.<sup>89,90</sup> Such mesh-type scaffolds have not been tested or optimized for osteoconduction, but only examined in view of their mechanics and stress shielding capabilities.

Numerous additively manufactured scaffolds have been produced from doped and nondoped bioglass. With a pore size of 0.25 mm, no significant difference was seen between filament-based lattice structures, oriented pore structures, and autologous bone in critical-size segmental defects in rat femora.<sup>91</sup> Similar results were achieved in an *in vivo* rabbit

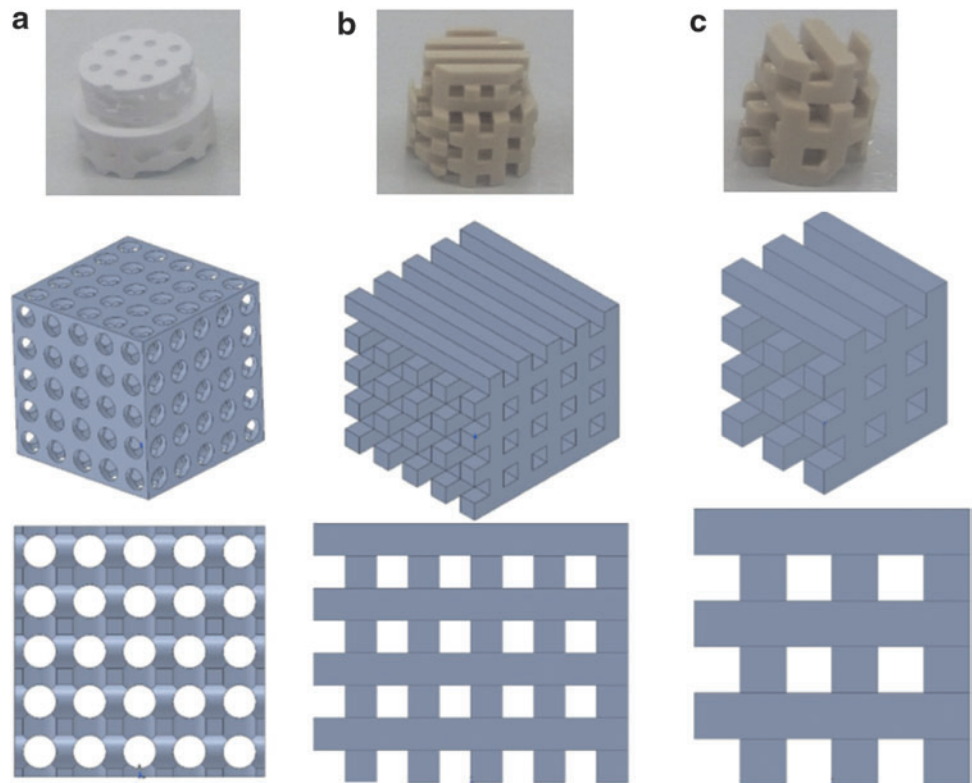


**FIG. 3.** Freely formed and filament-based implants and their designs. (a) A freely designed pore-based implant is shown. The drawing below represents a three-dimensional view of the design and in the lowest panel the view from the front. Respective views of filament-based designs are displayed from (b) a thin and (c) a twice as thick filament.



model with a filament-based lattice structure forming pores of  $0.15 \times 0.20$  mm.<sup>92</sup> These results show that such scaffolds can substitute for the use of autologous bone in critical-size defects. However, to date, wide-open microarchitectures with pores between 0.7 and 1.2 mm have not been tested.

In terms of bone ingrowth and osteoconduction in additive manufactured scaffolds, the majority of results are derived from scaffolds produced using filament-based methodologies (Fig. 3), since these machines are simpler and cheaper than most other systems. In a recent study, foamed and filament-based 3D-printed scaffolds from the same material were compared in femur defects in Beagle dogs. For both TCP-based scaffolds, the pore size varied in diameter between 0.227 mm for the foamed and 0.288 and 0.409 mm for the printer scaffolds. In terms of bone formation, the foamed scaffold performed significantly better.<sup>93</sup> In another study, filament-based scaffolds with channels of 0.10, 0.25, and 0.40 mm were tested in calvarial defects in mice. Here, scaffold

folds with 0.10 mm channels performed better than more open channels.<sup>94</sup> Because the defect only had a depth of 0.5 mm, the animal study design might have favored the smaller channels.

A more demanding radial diaphysis model in New Zealand white rabbits was applied with the result that the 3D-printed segmental bone substitute was superior to the solid block.<sup>95</sup> The first study comparing different microarchitectures with a filament-based extrusion system was undertaken with polycaprolactone (PCL)/TCP filaments with pores between 0.42 and 0.50 mm. Due to the filament thickness, the pore height was limited to 0.3 mm. Both microarchitectures varied in the orientation of the laydown patterns of the filaments, and *in vivo*, the scaffold with a  $0^\circ/90^\circ$  orientation performed better in terms of bone formation than the counterpart in which the filaments of the layers followed a  $0^\circ/60^\circ/120^\circ$ .<sup>96</sup> That the laydown pattern affects the mechanical strength of a scaffold was shown earlier.<sup>97</sup> Its influence on the osteoconduction of these two scaffolds

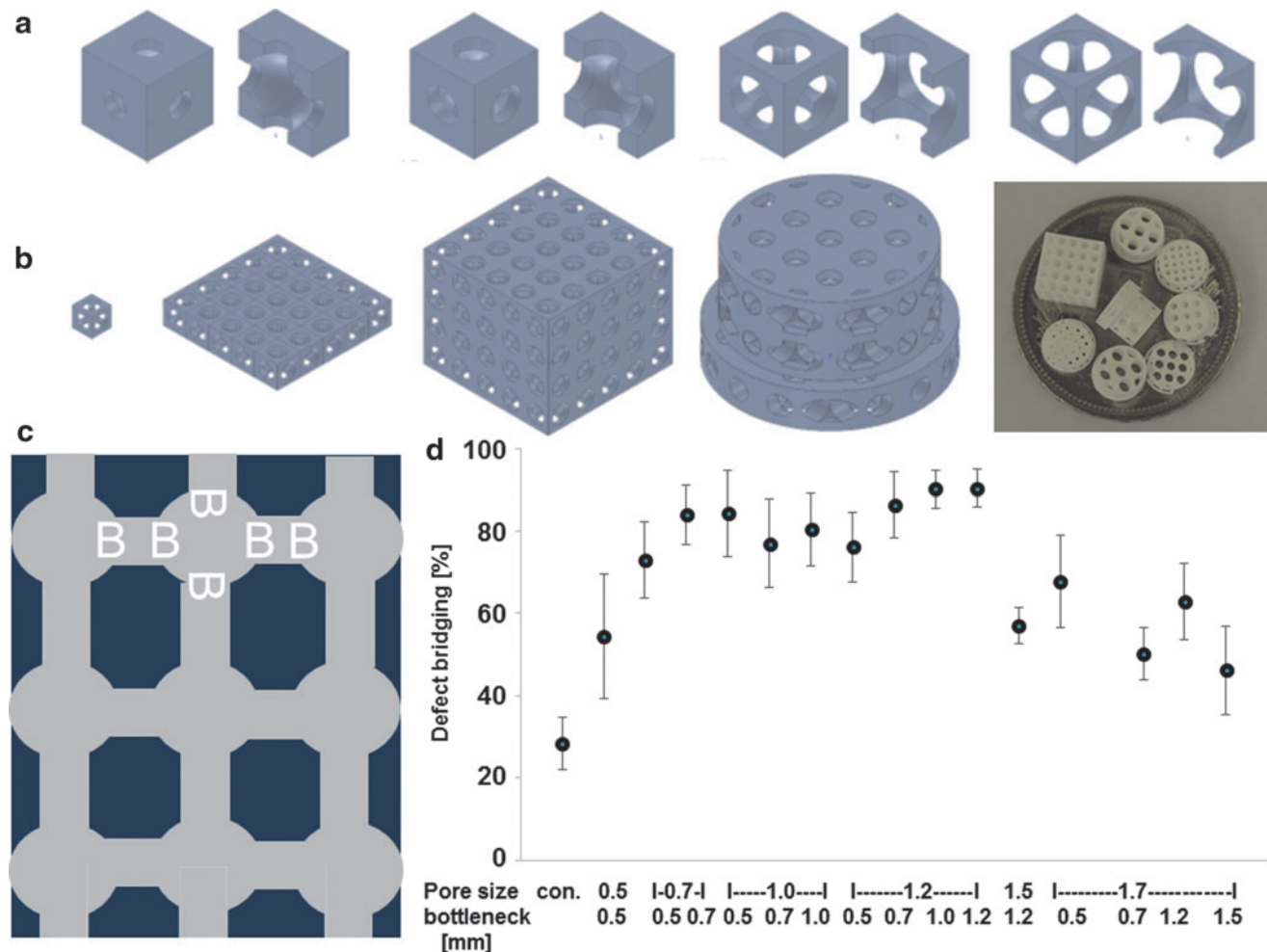
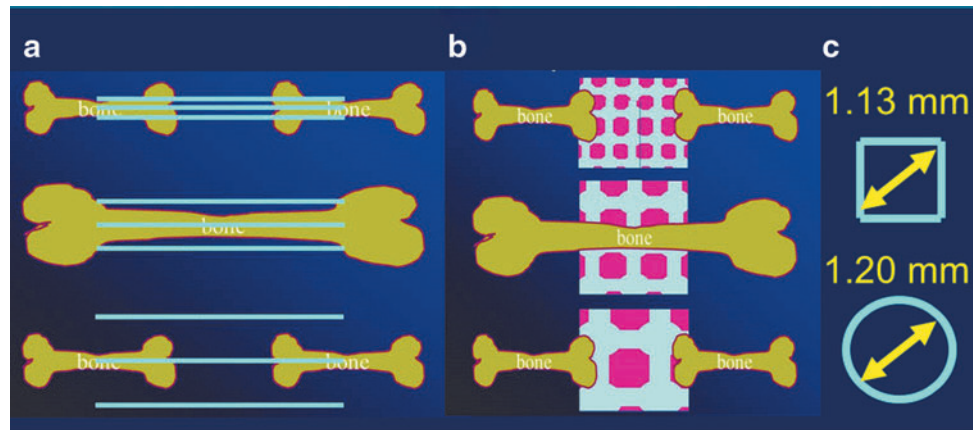


**FIG. 4.** Design and *in vivo* testing of TCP-based scaffolds. (a) Unit cell with increasing bottleneck. (b) Construction of scaffold for *in vivo* testing from unit cell to scaffolds displayed on a five Swiss Franc coin. (c) Pore distribution and bottleneck dimension (B) are shown. Scaffold is shown in dark blue, and pores are shown in gray. (d) Percentage of bony bridging of the defect in relation to pore and bottleneck dimensions. Compared with the empty control, scaffolds with pore diameters from 0.7 to 1.7 mm and bottlenecks <1.5 mm perform significantly better. Scaffolds with pores of 1.2 mm and bottlenecks between 0.7 and 1.2 perform significantly better than scaffolds with a pore diameter of 1.5 and bottleneck of 1.2 and with a pore diameter of 1.7 and bottleneck of 0.7. The results from each group are displayed as the mean  $\pm$  standard error of the mean. Data are drawn from Ghayor and Weber<sup>84</sup> with permission.



**FIG. 5.** Schematic drawing of osteoconductive microarchitectures. **(a)** In titanium-based lattice scaffolds, the optimal osteoconductive rod distance measures 0.8 mm. **(b)** For TCP-based porous scaffolds, the optimal osteoconductive pore diameter is 1.2 mm. **(c)** Because the rods form squares, the diagonal of the most osteoconductive squares and the most osteoconductive pore diameter are almost identical (1.13 and 1.20 mm, respectively).<sup>36,84</sup>



supports the notion that there is a tight relationship between microarchitecture and osteoconduction.

All the aforementioned studies, even when additive manufacturing was applied for production of the scaffolds, predominantly compared 1–3 scaffolds with “textbook” pore dimensions between 0.3 and 0.5 mm, which favors bone growth on the surface.<sup>35</sup> However, the search for highly osteoconductive microarchitectures should also include wide-open porous architectures. Such orthogonal periodic porous microarchitectures with pores of 1.75–2.5 mm were produced from PCL through additive manufacturing.<sup>98</sup> However, in the associated *in vivo* test, BMPs were applied, and the scaffolds were implanted subcutaneously. Therefore, these scaffolds were not tested for osteoconduction but for osteoinduction.

In 2018, the first library of narrow and wide-open lattice microarchitectures constructed from titanium was tested for osteoconduction in a calvarial defect model in rabbits. The outcome of this study revealed that the most osteoconductive lattice architecture is one consisting of rods with a thickness of 0.3 mm at a distance of 0.8 mm from each other.<sup>36</sup> To test the material dependence of this finding, microarchitecturally identical titanium and TCP scaffolds were compared, and no difference in the ingrowth of bone was found.<sup>99</sup> This is reasonable because with pores wider than 0.5 mm bone grows between the rods (Fig. 2), and therefore, bone growth may not be as dependent on the scaffold material,<sup>35</sup> as long as it maintains its osteoconductive guiding capability. However, the essence of this guiding capability is still elusive.

The most osteoconductive microarchitecture based on round pores connected by tubes (Fig. 4c) was identified with a library of 15 different scaffolds produced from TCP<sup>84</sup> (Fig. 4). Here, we found the best pore diameter to be 1.2 mm, performing significantly better than pores of  $\geq 1.5$  mm.<sup>84</sup> With highly osteoconductive wide-open porous microarchitectures with pores 1.2 mm in diameter, bony bridging reached  $90.4 \pm 4.5\%$  (mean  $\pm$  standard error of the mean [SEM]), a much higher value than that obtained with the 0.5 mm pores (consistent with the old dogma of the ideal pore diameter), yielding bony bridging of just  $54.4 \pm 15.2\%$  (mean  $\pm$  SEM). Therefore, wide-open porous microarchitectures with pores and bottlenecks between 0.7 and 1.2 mm in diameter appear to be highly osteoconductive.

The results from the osteoconductive lattice structure study determined in titanium-based scaffolds with an optimal rod

distance of 0.8 mm are almost superimposable with the ideal pore diameter of 1.2 mm found with TCP-based scaffolds, since the diagonal of such a square would measure 1.13 mm (Fig. 5). Therefore, these newly defined boundaries of 1.13–1.20 mm maximal distance between material surfaces for highly osteoconductive wide-open microarchitectures might be applicable to diverse materials and diverse microarchitectures. However, further studies are necessary to confirm or reject this hypothesis.

### Concluding Remarks

Since the 1990s, the excitement in the field of bone tissue engineering directed toward osteoinduction and the use of stem cells has hampered interest in applying and developing osteoconduction as another major driving force in bone regeneration. For spurious reasons and without systematic studies, mainly due to the lack of production methodologies, the field agreed on the optimal microarchitecture in terms of pore diameters for bone substitutes to be between 0.3 and 0.5 mm. In the meantime, new methodologies to freely design and realize microarchitectures in bone substitutes were developed, namely additive manufacturing. This new technology is a game changer not only in manufacturing of goods but also in our ability to freely design and produce new osteoconductive microarchitectures and test them *in vivo*.

Recent studies of porous structures increased the optimal pore size to 1.2 mm and the optimal osteoconductive lattice structure to rods of  $\sim 0.3$  mm in diameter and a spacing between rods of 0.8 mm. Both results translate to microarchitectures with a maximal optimal surface distance of 1.13–1.20 mm. Additive manufacturing will also be instrumental in studying the essence of osteoconduction. Already, wide-open porous microarchitectures could be realized through additive manufacturing, and osteoconductive bone ingrowth in those structures was shown to occur predominantly in the space between the material and not on the surface of the material forming the scaffold (Fig. 2). Therefore, these results support the early definition of osteoconduction as a 3D process of ingrowth of sprouting capillaries, perivascular tissue, and osteoprogenitor cells from a bony bed into the 3D structure of a porous implant (adjusted from Cornell and Lane<sup>9</sup>; Urist<sup>10</sup>) used as a guiding cue to bridge a defect with bony tissue. With this new tool of

additive manufacturing in hand, further studies on the essence of osteoconduction in terms of microarchitecture and guiding cues can be undertaken in the future.

In a recent commentary, it was postulated that “the ideal scaffold architecture does not exist, since each scaffold must fulfill several functions, such as resorption, bone ingrowth and mechanical support.”<sup>100</sup> Here, in this review, we only looked at microarchitecture and osteoconduction, and defined certain microarchitectures to be highly osteoconductive in terms of bony defect bridging.<sup>36,84</sup> Since bony defect bridging is the key element in avoiding nonunions, and given the clinical and economic burden of treating nonunions,<sup>101</sup> there is an obvious need to develop bone substitutes with high osteoconductive properties in terms of osteoconductive microarchitectures.

Based on this key input showing that osteoconductive microarchitectures avoid nonunions, materials must be developed for generation of new scaffold designs with the hope of meeting the mechanical and degradation needs and combining all these elements into one implant. Indisputably and in agreement with the comment,<sup>100</sup> this is a very tricky if not impossible task. However, dismissing the profound impact of scaffold microarchitecture on osteoconduction and the associated acceleration of bony bridging during bone regeneration would leave us with suboptimal bone substitutes. The alternative and more easily achievable approach would be to meet the mechanical needs independently of the bone substitute through conventional or even biodegradable osteosynthesis materials, such as plate and screw systems, and the bone substitute itself can be built by applying an optimally osteoconductive microarchitecture with well-known and well-established scaffold materials.

In essence, in the last 25 years, the field of bone tissue engineering followed the old rules for optimal microarchitectures of bone substitutes, forgot about the potential of osteoconduction, and focused predominantly on new, exciting developments, such as osteoinduction and the use of stem cells in bone repair. Now, with new technologies, such as additive manufacturing, in hand, we are able to design and realize an unlimited number of microarchitectures. This enables us to test these microarchitectures for osteoconduction and to define new boundaries for osteoconductive microarchitectures of bone substitutes, and thus further advance the field of bone tissue engineering through microarchitecturally designed, highly osteoconductive scaffolds alone or in combination with osteoinductive factors and/or stem cells.

### Acknowledgments

The author thanks Dr. Matthias Zehnder for critically reviewing the article, and Drs. Chafik Ghayor and Indranil Bhattacharya for editing the article. This work was supported by the Swiss National Science foundation through a grant to FEW (CR3213\_152809).

### Disclosure Statement

No competing financial interests exist.

### References

1. Meekeren, J.J. *Observationes Medicochirurgicae*. Amsterdam: Ex Officina Henrici & Vidnare Theodori, 1682.

2. Barth, A. *Histologische Untersuchungen über Knochenimplantationen*. Jena: Fischer, 1895.
3. Chase, S.W., and Herndon, C.H. The fate of autogenous and homogenous bone grafts: a historical review. *JBJS* **37**, 809, 1955.
4. Ollier, L. *Traite expérimental et clinique de la régénération des os et de la pilule artificielle du tissu osseux*. Paris: Victor Masson Et Fils, 1866.
5. Barth, A. *Ueber histologische Befunde nach Knochenimplantationen*. Jena: Fischer, 1893.
6. Phemister, D.B. Radium necrosis of bone. *Am J Roentgenol Radi* **16**, 340, 1926.
7. Axhausen, G. Histological studies on the cause and course of bone reconstruction in osteoplastic carcinoma. *Virchows Arch A* **195**, 358, 1909.
8. Turner, W.G. The use of the bone graft in surgery. *Can Med Assoc J* **5**, 103, 1915.
9. Cornell, C.N., and Lane, J.M. Current understanding of osteoconduction in bone regeneration. *Clin Orthop Relat Res* **355**, S267, 1998.
10. Urist, M.R. *Practical Applications of Basic Research on Bone Graft Physiology*. The American Academy of Orthopaedic Surgeons: Instructional Course Lectures. Saint Louis: The C. V. Mosby Company, 1976, p. 1.
11. Kruse, A., Jung, R.E., Nicholls, F., Zwahlen, R.A., Hammerle, C.H., and Weber, F.E. Bone regeneration in the presence of a synthetic hydroxyapatite/silica oxide-based and a xenogenic hydroxyapatite-based bone substitute material. *Clin Oral Implants Res* **22**, 506, 2011.
12. Schmidlin, P.R., Nicholls, F., Kruse, A., Zwahlen, R.A., and Weber, F.E. Evaluation of moldable, *in situ* hardening calcium phosphate bone graft substitutes. *Clin Oral Implants Res* **24**, 149, 2013.
13. Albrektsson, T., Branemark, P.I., Hansson, H.A., and Lindstrom, J. Osseointegrated titanium implants. Requirements for ensuring a long-lasting, direct bone-to-implant anchorage in man. *Acta Orthop Scand* **52**, 155, 1981.
14. Branemark, P.I., Hansson, B.O., Adell, R., *et al.* Osseointegrated implants in the treatment of the edentulous jaw—experience from a 10-year period. *Scand J Plast Recons* **16**, 1, 1977.
15. Albrektsson, T., and Johansson, C. Osteoinduction, osteoconduction and osseointegration. *Eur Spine J* **10**, S96, 2001.
16. Wennerberg, A., and Albrektsson, T. Effects of titanium surface topography on bone integration: a systematic review. *Clin Oral Implants Res* **20**, 172, 2009.
17. Wennerberg, A., and Albrektsson, T. On implant surfaces: a review of current knowledge and opinions. *Int J Oral Maxillofac Implants* **25**, 63, 2010.
18. Gittens, R.A., Olivares-Navarrete, R., Schwartz, Z., and Boyan, B.D. Implant osseointegration and the role of microroughness and nanostructures: lessons for spine implants. *Acta Biomater* **10**, 3363, 2014.
19. Kopf, B.S., Ruch, S., Berner, S., Spencer, N.D., and Maniura-Weber, K. The role of nanostructures and hydrophilicity in osseointegration: *in-vitro* protein-adsorption and blood-interaction studies. *J Biomed Mater Res A* **103**, 2661, 2015.
20. Kopf, B.S., Schipanski, A., Rottmar, M., Berner, S., and Maniura-Weber, K. Enhanced differentiation of human osteoblasts on Ti surfaces pre-treated with human whole blood. *Acta Biomater* **19**, 180, 2015.

21. Barradas, A.M.C., Yuan, H.P., van Blitterswijk, C.A., and Habibovic, P. Osteoinductive biomaterials: current knowledge of properties, experimental models and biological mechanisms. *Eur Cells Mater* **21**, 407, 2011.
22. Friedenstein, A.J., Petrakova, K.V., Kurolesova, A.I., and Frolova, G.P. Heterotopic of bone marrow. Analysis of precursor cells for osteogenic and hematopoietic tissues. *Transplantation* **6**, 230, 1968.
23. Levander, G. Tissue induction. *Nature* **155**, 148, 1945.
24. Levander, G., and Willstaedt, H. Alcohol-soluble osteogenic substance from bone marrow. *Nature* **157**, 587, 1946.
25. Urist, M.R. Bone: formation by autoinduction. *Science* **150**, 893, 1965.
26. Wozney, J.M., Rosen, V., Celeste, A.J., *et al.* Novel regulators of bone formation: molecular clones and activities. *Science* **242**, 1528, 1988.
27. Carragee, E.J., Hurwitz, E.L., and Weiner, B.K. A critical review of recombinant human bone morphogenetic protein-2 trials in spinal surgery: emerging safety concerns and lessons learned. *Spine J* **11**, 471, 2011.
28. Suzawa, M., Takeuchi, Y., Fukumoto, S., *et al.* Extracellular matrix-associated bone morphogenetic proteins are essential for differentiation of murine osteoblastic cells *in vitro*. *Endocrinology* **140**, 2125, 1999.
29. Ripamonti, U. Osteoinduction in porous hydroxyapatite implanted in heterotopic sites of different animal models. *Biomaterials* **17**, 31, 1996.
30. Reddi, A.H. Role of morphogenetic proteins in skeletal tissue engineering and regeneration. *Nat Biotechnol* **16**, 247, 1998.
31. Yuan, H., Fernandes, H., Habibovic, P., *et al.* Osteoinductive ceramics as a synthetic alternative to autologous bone grafting. *Proc Natl Acad Sci U S A* **107**, 13614, 2010.
32. LeGeros, R.Z. Calcium phosphate-based osteoinductive materials. *Chem Rev* **108**, 4742, 2008.
33. Ripamonti, U., Richter, P.W., and Thomas, M.E. Self-inducing shape memory geometric cues embedded within smart hydroxyapatite-based biomimetic matrices. *Plast Reconstr Surg* **120**, 1796, 2007.
34. Usas, A., and Huard, J. Muscle-derived stem cells for tissue engineering and regenerative therapy. *Biomaterials* **28**, 5401, 2007.
35. Kuboki, Y., Jin, Q., and Takita, H. Geometry of carriers controlling phenotypic expression in BMP-induced osteogenesis and chondrogenesis. *J Bone Joint Surg Am* **83-A**, S105, 2001.
36. de Wild, M., Ghayor, C., Zimmermann, S., *et al.* Osteoconductive lattice microarchitecture for optimized bone regeneration. *3D Print Addit Manuf* **6**, 2018; DOI: 10.1089/3dp.2017.0129.
37. Davies, J.E. Mechanisms of endosseous integration. *Int J Prosthodont* **11**, 391, 1998.
38. de Wild, M., Schumacher, R., Mayer, K., *et al.* Bone regeneration by the osteoconductivity of porous titanium implants manufactured by selective laser melting: a histological and micro computed tomography study in the rabbit. *Tissue Eng Part A* **19**, 2645, 2013.
39. Chia, H., and Wu, B. Recent advances in 3D printing of biomaterials. *J Biol Eng* **9**, 4, 2015.
40. Le Guehennec, L., Soueidan, A., Layrolle, P., and Amouriq, Y. Surface treatments of titanium dental implants for rapid osseointegration. *Dent Mater* **23**, 844, 2007.
41. de Wild, M., Zimmermann, S., Ruegg, J., *et al.* Influence of microarchitecture on osteoconduction and mechanics of porous titanium scaffolds generated by selective laser melting. *3D Print Addit Manuf* **3**, 142, 2016.
42. Goldberg, V.M., Stevenson, S., and Shaffer, J.W. In: Friedlaender, G.E., and Goldberg, V.M., eds. *Bone and Cartilage Allografts: Biology and Clinical Applications*. Park Ridge, IL: American Academy of Orthopedic Surgeons, 1991. p. 3.
43. Burchardt, H. The biology of bone graft repair. *Clin Orthop Relat Res* **174**, 28, 1983.
44. Guillemain, G., Patat, J.-L., Fournie, J., and Chetail, M. The use of coral as a bone graft substitute. *J Biomed Mater Res* **21**, 557, 1987.
45. Keaveny, T.M., Morgan, E.F., Niebur, G.L., and Yeh, O.C. Biomechanics of trabecular bone. *Annu Rev Biomed Eng* **3**, 307, 2001.
46. Egan, P.F., Gonella, V.C., Engensperger, M., Ferguson, S.J., and Shea, K. Computationally designed lattices with tuned properties for tissue engineering using 3D printing. *PLoS One* **12**, e0182902, 2017.
47. Kuboki, Y., Takita, H., Kobayashi, D., *et al.* BMP-induced osteogenesis on the surface of hydroxyapatite with geometrically feasible and nonfeasible structures: topology of osteogenesis. *J Biomed Mater Res* **39**, 190, 1998.
48. Karageorgiou, V., and Kaplan, D. Porosity of 3D biomaterial scaffolds and osteogenesis. *Biomaterials* **26**, 5474, 2005.
49. Bernstein, A., Niemeyer, P., Salzmann, G., *et al.* Microporous calcium phosphate ceramics as tissue engineering scaffolds for the repair of osteochondral defects: histological results. *Acta Biomater* **9**, 7490, 2013.
50. Polak, S.J., Rustom, L.E., Genin, G.M., Talcott, M., and Wagoner Johnson, A.J. A mechanism for effective cell-seeding in rigid, microporous substrates. *Acta Biomater* **9**, 7977, 2013.
51. Böhner, M., Baroud, G., Bernstein, A., *et al.* Characterization and distribution of mechanically competent mineralized tissue in micropores of  $\beta$ -tricalcium phosphate bone substitutes. *Mater Today* **20**, 106, 2017.
52. Hulbert, S.F., Young, F.A., Mathews, R.S., *et al.* Potential of ceramic materials as permanently implantable skeletal prostheses. *J Biomed Mater Res* **4**, 433, 1970.
53. Lapczynska, H., Galea, L., Wust, S., *et al.* Effect of grain size and microporosity on the *in vivo* behaviour of beta-tricalcium phosphate scaffolds. *Eur Cell Mater* **28**, 299, 2014.
54. Perez, R.A., and Mestres, G. Role of pore size and morphology in musculo-skeletal tissue regeneration. *Mater Sci Eng C* **61**, 922, 2016.
55. Tsuruga, E., Takita, H., Itoh, H., Wakisaka, Y., and Kuboki, Y. Pore size of porous hydroxyapatite as the cell-substratum controls BMP-induced osteogenesis. *J Biochem* **121**, 317, 1997.
56. Chang, B.S., Lee, C.K., Hong, K.S., *et al.* Osteoconduction at porous hydroxyapatite with various pore configurations. *Biomaterials* **21**, 1291, 2000.
57. Bobyn, J.D., Stackpool, G.J., Hacking, S., Tanzer, M., and Krygier, J.J. Characteristics of bone ingrowth and interface mechanics of a new porous tantalum biomaterial. *J Bone Joint Surg Br* **81**, 907, 1999.
58. Gauthier, O., Bouler, J.-M., Aguado, E., Pilet, P., and Daculsi, G. Macroporous biphasic calcium phosphate ce-

- ramics: influence of macropore diameter and macroporosity percentage on bone ingrowth. *Biomaterials* **19**, 133, 1998.
59. Fisher, J.P., Vehof, J.W., Dean, D., *et al.* Soft and hard tissue response to photocrosslinked poly(propylene fumarate) scaffolds in a rabbit model. *J Biomed Mater Res* **59**, 547, 2002.
  60. Chang, B., Song, W., Han, T., *et al.* Influence of pore size of porous titanium fabricated by vacuum diffusion bonding of titanium meshes on cell penetration and bone ingrowth. *Acta Biomater* **33**, 311, 2016.
  61. Gui, N., Xu, W., Myers, D.E., Shukla, R., Tang, H.P., and Qian, M. The effect of ordered and partially ordered surface topography on bone cell responses: a review. *Biomater Sci* **6**, 250, 2018.
  62. Azeem, A., English, A., Kumar, P., *et al.* The influence of anisotropic nano- to micro-topography on *in vitro* and *in vivo* osteogenesis. *Nanomedicine (Lond)* **10**, 693, 2015.
  63. Hefti, T., Frischherz, M., Spencer, N.D., Hall, H., and Schlottig, F. A comparison of osteoclast resorption pits on bone with titanium and zirconia surfaces. *Biomaterials* **31**, 7321, 2010.
  64. von Doernberg, M.-C., von Rechenberg, B., Böhner, M., *et al.* *In vivo* behavior of calcium phosphate scaffolds with four different pore sizes. *Biomaterials* **27**, 5186, 2006.
  65. Feng, Y.-F., Wang, L., Li, X., *et al.* Influence of architecture of  $\beta$ -tricalcium phosphate scaffolds on biological performance in repairing segmental bone defects. *PLoS One* **7**, e49955, 2012.
  66. Hutmacher, D.W. Scaffolds in tissue engineering bone and cartilage. *Biomaterials* **21**, 2529, 2000.
  67. Hutmacher, D.W., and Cool, S. Concepts of scaffold-based tissue engineering—the rationale to use solid free-form fabrication techniques. *J Cell Mol Med* **11**, 654, 2007.
  68. Jariwala, S.H., Lewis, G.S., Bushman, Z.J., Adair, J.H., and Donahue, H.J. 3D printing of personalized artificial bone scaffolds. *3D Print Addit Manuf* **2**, 56, 2015.
  69. Sears, N.A., Seshadri, D.R., Dhavalikar, P.S., and Cosgriff-Hernandez, E. A review of three-dimensional printing in tissue engineering. *Tissue Eng Part B Rev* **22**, 298, 2016.
  70. Carrel, J.P., Wiskott, A., Moussa, M., Rieder, P., Scherrer, S., and Durual, S. A 3D printed TCP/HA structure as a new osteoconductive scaffold for vertical bone augmentation. *Clin Oral Implants Res* **27**, 55, 2016.
  71. Seitz, H., Rieder, W., Irsen, S., Leukers, B., and Tille, C. Three-dimensional printing of porous ceramic scaffolds for bone tissue engineering. *J Biomed Mater Res B Appl Biomater* **74**, 782, 2005.
  72. Brunello, G., Sivoletta, S., Meneghello, R., *et al.* Powder-based 3D printing for bone tissue engineering. *Biotechnol Adv* **34**, 740, 2016.
  73. Sachs, E., Cima, M., and Cornie, J. Three-dimensional printing: rapid tooling and prototypes directly from a CAD model. *CIRP Ann Manuf Technol* **39**, 201, 1990.
  74. Butscher, A., Böhner, M., Doebelin, N., Hofmann, S., and Müller, R. New depowdering-friendly designs for three-dimensional printing of calcium phosphate bone substitutes. *Acta Biomater* **9**, 9149, 2013.
  75. Butscher, A., Böhner, M., Roth, C., Ernstberger, A., Heuberger, R., and Doebelin, N. Printability of calcium phosphate powders for three-dimensional printing of tissue engineering scaffolds. *Acta Biomater* **8**, 373, 2012.
  76. Crump, S.S. Apparatus and method for creating tree-dimensional objects. Patent No. 5121329, 1992.
  77. Millán, A.J., Santacruz, I., Sánchez-Herencia, A.J., Nieto, M.I., and Moreno, R. Gel-extrusion: a new continuous forming technique. *Adv Eng Mater* **4**, 913, 2002.
  78. Vozzi, G., Previti, A., De Rossi, D., and Ahluwalia, A. Microsyringe-based deposition of two-dimensional and three-dimensional polymer scaffolds with a well-defined geometry for application to tissue engineering. *Tissue Eng* **8**, 1089, 2002.
  79. Hutmacher, D.W., Schantz, T., Zein, I., Ng, K.W., Teoh, S.H., and Tan, K.C. Mechanical properties and cell cultural response of polycaprolactone scaffolds designed and fabricated via fused deposition modeling. *J Biomed Mater Res* **55**, 203, 2001.
  80. Schantz, J.T., Lim, T.C., Ning, C., *et al.* Cranioplasty after trephination using a novel biodegradable burr hole cover: technical case report. *Neurosurgery* **58**, 2006; DOI: 10.1227/01.NEU.0000193533.54580.3F.
  81. Schwentenwein, M., and Homa, J. Additive manufacturing of dense alumina ceramics. *Int J Appl Ceram Tec* **12**, 1, 2015.
  82. Roy, T.D., Simon, J.L., Ricci, J.L., Rekow, E.D., Thompson, V.P., and Parsons, J.R. Performance of degradable composite bone repair products made via three-dimensional fabrication techniques. *J Biomed Mater Res A* **66**, 283, 2003.
  83. Dutta Roy, T., Simon, J.L., Ricci, J.L., Rekow, E.D., Thompson, V.P., and Parsons, J.R. Performance of hydroxyapatite bone repair scaffolds created via three-dimensional fabrication techniques. *J Biomed Mater Res Part A* **67A**, 1228, 2003.
  84. Ghayor, C., and Weber, F.E. Osteoconductive micro-architecture of bone substitutes for bone regeneration revisited. *Front Physiol* **9**, 960, 2018.
  85. Li, J.P., Habibovic, P., van den Doel, M., *et al.* Bone ingrowth in porous titanium implants produced by 3D fiber deposition. *Biomaterials* **28**, 2810, 2007.
  86. Taniguchi, N., Fujibayashi, S., Takemoto, M., *et al.* Effect of pore size on bone ingrowth into porous titanium implants fabricated by additive manufacturing: an *in vivo* experiment. *Mater Sci Eng C* **59**, 690, 2016.
  87. Ran, Q., Yang, W., Hu, Y., *et al.* Osteogenesis of 3D printed porous Ti6Al4V implants with different pore sizes. *J Mech Behav Biomed Mater* **84**, 1, 2018.
  88. Obaton, A.F., Fain, J., Djemaï, M., *et al.* *In vivo* XCT bone characterization of lattice structured implants fabricated by additive manufacturing. *Heliyon* **3**, e00374, 2017.
  89. Pobloth, A.-M., Checa, S., Razi, H., *et al.* Mechanobiologically optimized 3D titanium-mesh scaffolds enhance bone regeneration in critical segmental defects in sheep. *Sci Transl Med* **10**, eaam8828, 2018.
  90. Razi, H., Checa, S., Schaser, K.-D., and Duda, G.N. Shaping scaffold structures in rapid manufacturing implants: a modeling approach toward mechano-biologically optimized configurations for large bone defect. *J Biomed Mater Res Part B Appl Biomater* **100B**, 1736, 2012.
  91. Bi, L., Zobel, B., Liu, X., Rahaman, M.N., and Bonewald, L.F. Healing of critical-size segmental defects in rat femora using strong porous bioactive glass scaffolds. *Mater Sci Eng C* **42**, 816, 2014.
  92. Jia, W., Lau, G.Y., Huang, W., Zhang, C., Tomsia, A.P., and Fu, Q. Bioactive glass for large bone repair. *Adv Healthc Mater* **4**, 2842, 2015.
  93. Barba, A., Maazouz, Y., Diez-Escudero, A., *et al.* Osteogenesis by foamed and 3D-printed nanostructured calcium



- phosphate scaffolds: effect of pore architecture. *Acta Biomater* **79**, 135, 2018.
94. Diao, J., OuYang, J., Deng, T., *et al.* 3D-plotted beta-tricalcium phosphate scaffolds with smaller pore sizes improve *in vivo* bone regeneration and biomechanical properties in a critical-sized calvarial defect rat model. *Adv Healthc Mater* **7**, e1800441, 2018.
  95. Tovar, N., Witek, L., Atria, P., *et al.* Form and functional repair of long bone using 3D-printed bioactive scaffolds. *J Tissue Eng Regen Med* **12**, 1986, 2018.
  96. Berner, A., Woodruff, M.A., Lam, C.X., *et al.* Effects of scaffold architecture on cranial bone healing. *Int J Oral Maxillofac Surg* **43**, 506, 2014.
  97. Zein, I., Huttmacher, D.W., Tan, K.C., and Teoh, S.H. Fused deposition modeling of novel scaffold architectures for tissue engineering applications. *Biomaterials* **23**, 1169, 2002.
  98. Williams, J.M., Adewunmi, A., Schek, R.M., *et al.* Bone tissue engineering using polycaprolactone scaffolds fabricated via selective laser sintering. *Biomaterials* **26**, 4817, 2005.
  99. Chen, T.H., Ghayor, C., Siegenthaler, B., *et al.* Lattice microarchitecture for bone tissue engineering from calcium phosphate compared to titanium. *Tissue Eng Part A* **24**, 1554, 2018.
  100. Bohner, M., Loosli, Y., Baroud, G., and Lacroix, D. Commentary: deciphering the link between architecture and biological response of a bone graft substitute. *Acta Biomater* **7**, 478, 2011.
  101. Zura, R., Xiong, Z., Einhorn, T., *et al.* Epidemiology of fracture nonunion in 18 human bones. *JAMA Surg* **151**, e162775, 2016.

Address correspondence to:

*Franz E. Weber, PhD*

*Oral Biotechnology and Bioengineering*

*Center for Dental Medicine*

*Department of Cranio-Maxillofacial and Oral Surgery*

*University of Zürich*

*Plattenstrasse 11*

*Zürich 8032*

*Switzerland*

*E-mail: franz.weber@zzm.uzh.ch*

*Received: February 11, 2019*

*Accepted: April 17, 2019*

*Online Publication Date: August 19, 2019*